3D Well-composed Polyhedral Complexes

Rocio Gonzalez-Diaz[1], Maria-Jose Jimenez[1], Belen Medrano

Applied Math Department, University of Seville,

Av. Reina Mercedes, s/n, Seville, Spain

e-mails: {rogodi,majiro,belenmg}@us.es

March 13, 2014

Abstract

A binary three-dimensional (3D) image I is well-composed if the boundary surface of its continuous analog is a 2D manifold. Since 3D images are not often well-composed, there are several voxel-based methods ("repairing" algorithms) for turning them into well-composed ones but these methods either do not guarantee the topological equivalence between the original image and its corresponding well-composed one or involve sub-sampling the whole image. In this paper, we present a method to locally "repair" the cubical complex $Q(I)$ (embedded in $\mathbb{R}^3$) associated to I to obtain a polyhedral complex $P(I)$ homotopy equivalent to $Q(I)$ such that the boundary of every connected component of $P(I)$ is a 2D manifold. The reparation is performed via a new codification system for $P(I)$ under the form of a 3D grayscale image that allows an efficient access to cells and their faces.

Keywords: binary 3D image, well-composedness, cubical complex, polyhedral complex, homotopy equivalence, 2D manifold

1   Introduction

3D well-composed images [14] enjoy important topological and geometrical properties in such a way that several algorithms used in computer vision, computer graphics and image processing are simpler. For example, thinning algorithms can be simplified and naturally made parallel if the input image

is well-composed [13, 17]; some algorithms for computing surface curvature or extracting adaptive triangulated surfaces assume that the input image is well-composed [11]. However, our main motivation is that of (co)homology computations on the cell complex representing the 3D image [6, 7]. We could take advantage of a well-composed-like representation since computations could be performed only on the boundary subcomplex.

Since 3D images are often not well-composed, there are several methods (repairing algorithms) for turning them into well-composed ones [15, 21], but these methods do not guarantee the topological equivalence between the original and its corresponding well-composed image. In fact, the purpose may even be to simplify as much as possible the topology (in the sense of removing little topological artifacts). However, we are concerned with the fact of preserving the topology of the input image having in mind cases in which subtle details may be important.

In [18], the authors provide a solution to the problem of topology preservation during digitization of 3D objects. They use several reconstruction methods that all result in a 3D object with a 2D manifold surface. More specifically, one of the proposed methods is a voxel-based method called Majority Interpolation, by which resolution is doubled in any direction and new sampling voxels are added to the foreground under some constraints. Other method is based on the most common reconstruction methods for 3D digital images is the marching cube (MC) algorithm [16] which analyzes local configurations of eight neighboring sampling points in order to reconstruct a polygonal surface. There even exists a MC variant, called asymmetric marching cubes, which generates the reconstruction of manifold surfaces (see [19, page 101]). A different approach is made in [12], where the authors create a polyhedral complex as the continuous analog of a set of voxels with given digital adjacencies. They also show that such a continuous analog corresponds to the usual definition of iso-surface in the $3D$ case.

In our approach, we first consider a a cubical complex $Q(I)$ associated to a voxel-based representation of the given image I. Then, we develop a new scheme of representation, called ExtendedCubeMap (ECM) representation, based on a 3D grayscale image storing the cells and the boundary face relations of cells of $Q(I)$. Working on an ECM representation of $Q(I)$, we design a procedure to obtain a polyhedral complex $P(I)$ homotopy equivalent to $Q(I)$. The importance of our method is that the cells of $P(I)$ are totally encoded in a 3D grayscale image g_P, and their boundary face relations in a set of structuring elements B_P. It is worth to mention that the set B_P remains

2

the same for any polyhedral complex $P(I)$ computed using our method.

In our prequel paper [8], the complex $P(I)$ homotopy equivalent to $Q(I)$, was a cell complex constructed with more general building blocks than polyhedra depending on the local configuration of voxels. In this paper, $P(I)$ is always a polyhedral complex, constructed with a general procedure (that is valid for all the local configurations), with the advantage that it can be stored in a matrix form (a 3D grayscale image) in a way that we do not need to build $P(I)$ to obtain face relations between its cells.

Section 2 is devoted to clarify, first, the correspondence between 3D binary digital images and cubical complexes; the notion of well-composedness is also introduced as well as its extension to complete polyhedral complexes. Section 3 describes a new codification system called ECM representation of cubical complexes which is also valid for other more general polyhedral complexes as we will see later in this paper. Section 4 describes the repairing algorithm to get a well-composed polyhedral complex, $P(I)$, starting from the cubical complex $Q(I)$ associated to a non-well-composed image I. The repairing process is, in fact, accomplished on the ECM representation E_Q of $Q(I)$ to get the ECM representation E_P of $P(I)$. Finally, we draw some conclusions and statements for future work in the last section.

2 3D Images, Polyhedral Complexes and Well-composedness

Consider $\mathbb{Z}^3$ as the set of points with integer coordinates in 3D space $\mathbb{R}^3$. A *3D binary digital image* (or 3D image for short) is a set $I = (\mathbb{Z}^3, 26, 6, B)$ (or $I = (\mathbb{Z}^3, B)$, for short), where $B \subset \mathbb{Z}^3$ is the *foreground*, $B^c = \mathbb{Z}^3 \backslash B$ the *background*, and $(26, 6)$ is the adjacency relation for the foreground and background, respectively. A point of $\mathbb{Z}^3$ can be interpreted as a unit closed cube (called *voxel*) in $\mathbb{R}^3$ centered at the point and with faces parallel to the coordinate planes. The set of voxels centered at the points of B in $\mathbb{R}^3$ is called the *continuous analog* of I and it is denoted by $C(I)$. The *boundary surface* of $C(I)$ is the set of points in $\mathbb{R}^3$ that are shared by the voxels centered at points of B and those centered at points of B^c (see [1, 5, 20]).

Recall that a 3D image $I = (\mathbb{Z}^3, B)$ is *well-composed* [14] if the *boundary surface* of $C(I)$ is a 2D manifold, i.e. each point has a neighborhood homeomorphic to $\mathbb{R}^2$ (it "looks" locally like a planar open set). The set of

voxels of $C(I)$, together with all their faces (squares, edges and vertices) and the coface relationship between them, constitute a combinatorial structure called *cubical complex*, denoted by $Q(I)$ whose geometric realization is exactly $C(I)$. The topology of $Q(I)$ reflects the topology of I whenever $(26,6)$−adjacency is considered on I. This way, we will say that the cubical complex $Q(I)$ associated to a 3D image I is well-composed if the corresponding image I is well-composed. Considering configurations of 8 cubes sharing a vertex, one finds eleven different 8−cube configurations (modulo reflections and 90−degree rotations) around a critical vertex, as showed in Fig. 1, where well-composedness condition is not satisfied. For the eleven 8−cube configurations, the central vertex v is a *critical vertex* in the sense that it does not have a neighborhood in the boundary surface of $Q(I)$, homeomorphic to $\mathbb{R}^2$. These eleven 8−cube configurations come exactly from the $(2 \times 2 \times 2)$−configurations which contain one of the just two configurations being presented in [14, Fig. 3]. A cubical complex is a specific type of *polyhedral complex* (see [10]). A polyhedral complex K is a combinatorial structure by which a space is decomposed into vertices, edges, polygons and polyhedra (cells, in general) that are glued together by their boundaries such that the intersection of any two cells of the complex is also a cell of the complex. Notice that the structure of a polyhedral complex K can be considered as purely combinatorial (i.e., a set of cells with coface relations between them), but in this work, it is associated to a specific geometric realization of K in $\mathbb{R}^3$.

The dimension of an i−cell $\sigma \in K$ is $dim(\sigma) = i$. A cell $\mu \in K$ is a *face* of a cell $\sigma \in K$ if μ lies in the boundary of σ and $dim(\mu) \leq dim(\sigma)$. The cell σ is called a *coface* of μ. A cell μ is *maximal* if it is not a face of any other cell $\sigma \in K$ and *free* if it is face of exactly one maximal cell of K. The *boundary subcomplex* ∂K is made up by the free cells of K, together with all their faces. The *closure* of a subset S of K is the smallest subcomplex of K that contains each cell in S. It is obtained by repeatedly adding to S each face of every cell in S. The *star of S* (denoted $St\,S$) is the set of all cells in K that have any faces in S. Note that the star is generally not a cell complex itself. The *link of S* (denoted by $Lk\,S$) is the closure of the star of S minus the star of all faces of S. K is an nD polyhedral complex if for any cell $\sigma \in K$, $dim(\sigma) \leq n$ and for some maximal cell $\mu \in K$, $dim(\mu) = n$. An nD polyhedral complex is *complete* if all its maximal cells have dimension n.

Observe that if K is complete, so it is ∂K. In particular, the cubical complex associated to an image I, $Q(I)$, and its boundary subcomplex, $\partial Q(I)$,
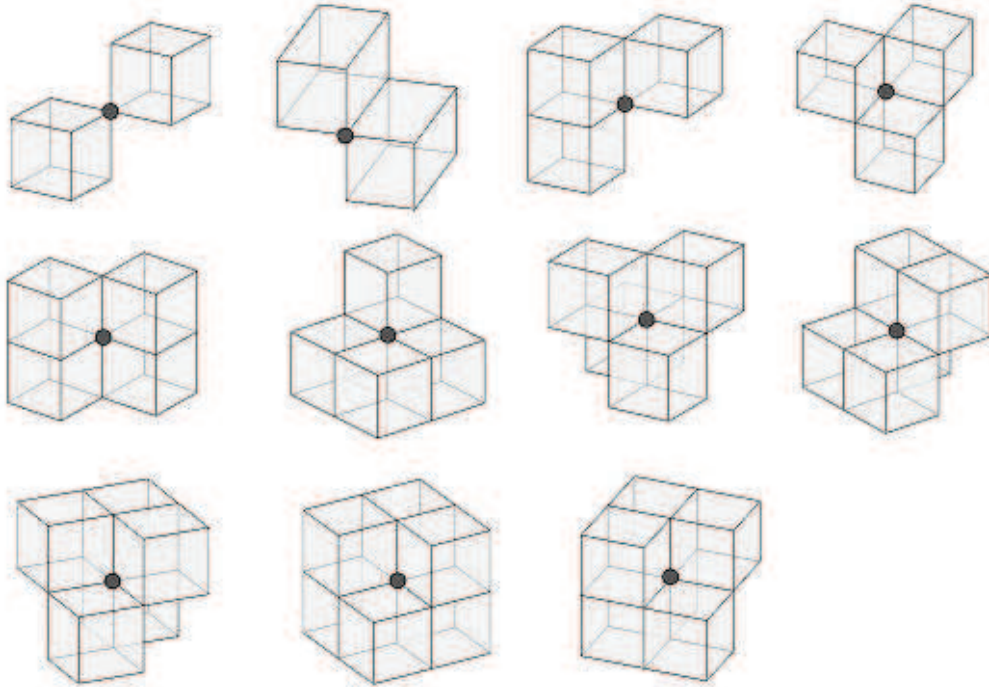
Figure 1: The eleven 8−cube configurations around a critical vertex.

are, respectively, 3D and 2D complete polyhedral complexes.

The following definition extends the notion of well-composedness to 3D complete polyhedral complexes.

Definition 1. *A 3D complete polyhedral complex K embedded in $\mathbb{R}^3$ is well-composed if the subcomplex ∂K is a disconnected union of 2D manifolds.*

Proposition 1. *A 3D complete polyhedral complex K is well-composed if the subcomplex ∂K satisfies that:*

(E1) any edge has exactly two 2-cofaces in ∂K;

(E2) for any vertex $v \in \partial K$, $Lk\{v\}$ in ∂K has exactly one connected component.

Proof. Take a point $p \in \partial K$. Recall that ∂K is made up by a set of 2−cells, together with all their faces. If p lies inside a 2−cell in ∂K, obviously the proposition holds; if p lies on an edge $e \in \partial K$, condition $E1$ applies and

5

hence the proposition holds, too; if p is a vertex of ∂K, the star of p in ∂K, is homeomorphic to a disk (thanks to conditions $E1$ and $E2$). $\square$

Notice that conditions $E1$ and $E2$ are not satisfied (simultaneously) in the configurations showed in Fig. 1.

Definition 2. *Given a 3D complete polyhedral complex K embedded in $\mathbb{R}^3$, a vertex v is critical if either $E1$ fails for some $1-$coface of v or $E2$ is not satisfied by v. Then, K is well-composed if there is not any critical vertex in ∂K.*

An alternative definition of well-composedness has been presented in [19, page 11] based on adjacency of maximal cells. In this paper, we use the one involving the notion of critical vertex given above since the repairing process is done on that vertices and their stars.

3   ExtendedCubeMap Representation

In [2], the authors presented a data-structure (called *CubeMap representation*) designed to compactly store and quickly manipulate cubical complexes. A similar structure was first introduced in CAPD library [3] for computing cubical homology. In that representation, for each cube (voxel), vertices, edges, squares and the cube itself were encoded in a $3 \times 3 \times 3$ array with values representing the dimension of each cell (see Fig. 2.c). For a set of voxels, the corresponding array is composed by overlapping copies of arrays of size $3 \times 3 \times 3$. The CubeMap representation is, in fact, a 3D generalization of the Khalimsky grid, which has already been introduced and extensively used by V. Kovalevsky (e.g. in [9]).

Inspired by that representation scheme, we define a new data-structure, called ExtendedCubeMap representation, that allows to store not only 3D cubical complexes but also the new polyhedral complexes that will be constructed. This new codification is still presented under a 3D array form, also encoding the dimension of the cells that are represented (that is, a 3D grayscale image). In such a structure, the information of boundary relations between represented cells will be extracted by searching for certain structuring elements inside the representation.

An *nD grayscale image* is a map $g : \mathbb{Z}^n \to \mathbb{Z}$. Given a point $p \in \mathbb{Z}^n$, $g(p)$ is referred to as the *color* of p. A *structuring element* is also an nD

grayscale image $b : D_b \subseteq \mathbb{Z}^n \to \mathbb{Z}$ whose domain contains the origin $o \in D_b$. A structuring element will be used to perform a given operation around a certain neighborhood of a point.

Definition 3. *Given an nD complete polyhedral complex K, an Extended-CubeMap (ECM) representation of K is a triple $E_K = (h_K, g_K, B_K)$ where:*

- $h_K : D_K \to K$ *is a bijective function, for a certain domain $D_K \subset \mathbb{Z}^n$ with as many points as cells in K. For each cell σ, denote by p_σ the point $h_K^{-1}(\sigma)$ representing σ;*

- $g_K : \mathbb{Z}^n \to \{-1, 0, 1, \dots, n\}$ *is an nD grayscale image, such that:*

    - $g_K(p) = dim(h_K(p))$, *for any $p \in D_K$, .*
    - $g_K(p) = -1$, *For any $p \in \mathbb{Z}^n \setminus D_K$.*

- B_K *is a set of structuring elements $\{b : D_b \subset \mathbb{Z}^n \to \mathbb{Z}\}$ such that for any $i-$cell $\sigma \in K$, there exists a single structuring element $b_\sigma : D_\sigma \to \mathbb{Z}$ in B_K such that:*

    - $b_\sigma(p) = g_K(p + p_\sigma)$, *for any $p \in D_\sigma$. In particular, $b_\sigma(o) = i$;*
    - *If $p \in D_\sigma$ and $p \neq o$ then either $b_\sigma(p) = i - 1$ or $b_\sigma(p) = -1$;*
    - *A point $p \in \mathbb{Z}^3$ satisfies that $p - p_\sigma \in D_\sigma$ and $b_\sigma(p - p_\sigma) = i - 1$ if and only if p represents a cell μ (that is, $p = h_K^{-1}(\mu)$) which is an $(i-1)-$face of σ.*

Remark 1. *In order to visualize examples of ECM representations, from now on, a point $p \in \mathbb{Z}^3$ is colored black if $g_Q(p) = 3$, green if $g_Q(p) = 2$, red if $g_Q(p) = 1$, blue if $g_Q(p) = 0$ and white if $g_Q(p) = -1$. For a better understanding of the pictures, the reader is referred to the web version of this paper.*

An ECM representation of K may not exist and may not be unique (see, for example, Fig. 2.(c,d) which shows two different ECM representations of a single cube together with all its faces). Nevertheless, given a cubical complex $Q(I)$ and the ECM representation E_Q of $Q(I)$ given in Prop. 2, the procedures described in the next section will provide a unique polyhedral complex $P(I)$ as well as a unique ECM representation E_P of $P(I)$.

Since the map h_K is bijective, each cell $\sigma \in K$ is represented by a single point $p_\sigma = h_K^{-1}(\sigma) \in \mathbb{Z}^n$. Moreover, for each $p \in D_K$, $g_K(p)$ codifies the
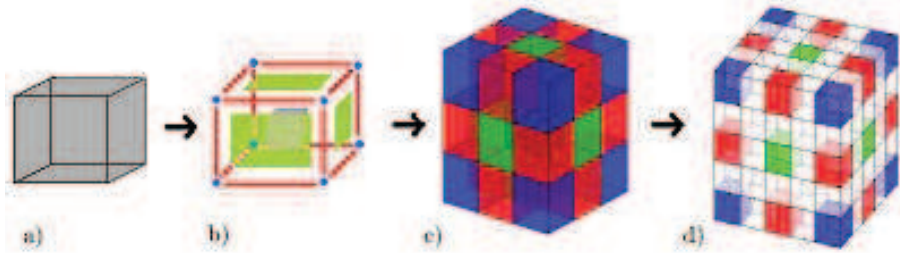
Figure 2: a) A single voxel I; b) the cubical complex $Q(I)$ associated to I; c) The color values in the CubeMap representation of $Q(I)$ which is also an ECM representation of $Q(I)$; d) The color values in the ECM representation E_Q of $Q(I)$. In both c) and d) the central voxel is colored black.

dimension of the cell in K that p represents (that is, the cell $\sigma = h_K(p)$). Finally, observe that the structuring element $b_\sigma : D_\sigma \to \mathbb{Z}$ associated to a cell $\sigma \in K$ provides a codification of the boundary face relations for σ. Therefore, within this codification system, the extraction of boundary faces of any cell σ can be done by checking if any of the structuring elements of B_K fits around the point p_σ (that is, the point in D_K that represents σ). This last operation could be seen as a morphological erosion of the 3D grayscale image g_K by the corresponding structuring element.

Definition 4. *Given an ECM representation $E_K = (h_K, g_K, B_K)$ of a polyhedral complex K, a structuring element $b : D_b \to \mathbb{Z}$ is said to fit around a point $p \in D_K \subset \mathbb{Z}^n$ if, for any $q \in D_b$, $g_K(p + q) = b(q)$.*

Fig. 3 shows an example of a polyhedral complex K, the color values in an ECM representation E_K of K and the structuring elements (modulo $90-$degree rotations) associated to the cells of K.

The following result provides an ECM representation of a cubical complex $Q(I)$ associated to a 3D image I. Let r_σ be the barycenter of $\sigma \in Q(I)$ and $D_Q = \{p \in \mathbb{Z}^3$ such that $p = 4r_\sigma$ for some $\sigma \in Q(I)\}$.

Proposition 2. *Let $Q(I)$ be the cubical complex associated to a 3D image I, the triple $E_Q = (h_Q, g_Q, B_Q)$ described below is an ECM representation of $Q(I)$.*

- *$h_Q : D_Q \to Q(I)$, where:*

    - *$D_Q = \{p \in \mathbb{Z}^3$ such that $p = 4r_\sigma$ for some $\sigma \in Q(I)\}$;*
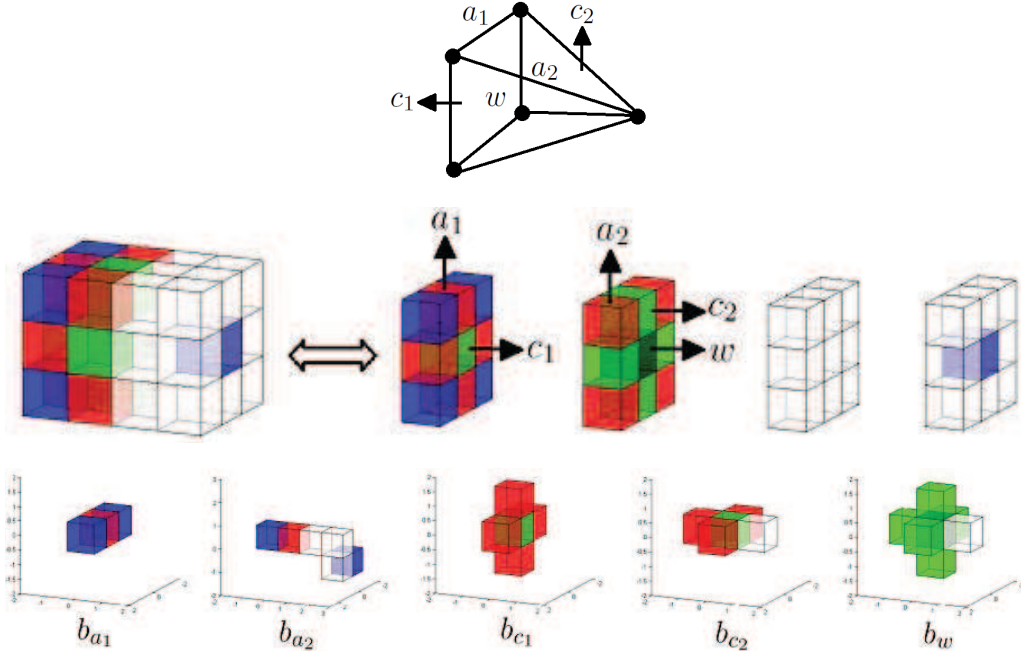
8

Figure 3: Top: A polyhedral complex K (a solid pyramid). Middle: The color values of the voxels in an ECM representation of K. Bottom: Structuring elements (modulo 90−degree rotations) associated to the cells of K.

- $h_Q(4r_\sigma) = \sigma$ for $\sigma \in Q(I)$;

- $g_Q : \mathbb{Z}^3 \to \{-1, 0, 1, 2, 3\}$ is given by $g_Q(p) = dim(\sigma)$ if $p = 4r_\sigma \in D_Q$, and $g_Q(p) = -1$ otherwise. See Fig. 2.d;

- $B_Q = \{b_\ell : D_\ell \to \mathbb{Z}\}_{\ell=1,2,3}$, where $b_\ell : D_\ell \to \mathbb{Z}$ (modulo 90−degree rotations) is given by:

  - $D_1 = \{o, (\pm 1, 0, 0), (\pm 2, 0, 0)\}$, $b_1(o) = 1$, $b_1(p) = 0$ for $p = (\pm 2, 0, 0)$ and $b_1(p) = 0$ otherwise. See Fig. 4.x;

  - $D_2 = \{o, (\pm 1, 0, 0), (0, \pm 1, 0), (\pm 2, 0, 0), (0, \pm 2, 0)\}$, $b_2(o) = 2$, $b_2(p) = 1$ for $p = (\pm 2, 0, 0), (0, \pm 2, 0)$ and $b_2(p) = -1$ otherwise. See Fig. 5.x;

  - $D_3 = \{o, (\pm 1, 0, 0), (0, \pm 1, 0), (0, 0, \pm 1), (\pm 2, 0, 0), (0, \pm 2, 0), (0, 0, \pm 2)\}$, $b_3(o) = 3$, $b_3(p) = 2$ for $p = (\pm 2, 0, 0), (0, \pm 2, 0), (0, 0, \pm 2)$ and $b_3(p) = -1$ otherwise. See Fig. 6.x.
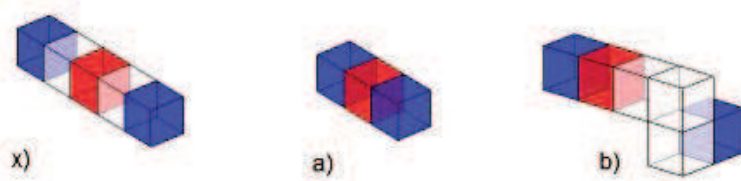
9

Figure 4: Structuring elements that provide boundary face relations between edges and their 0−faces.
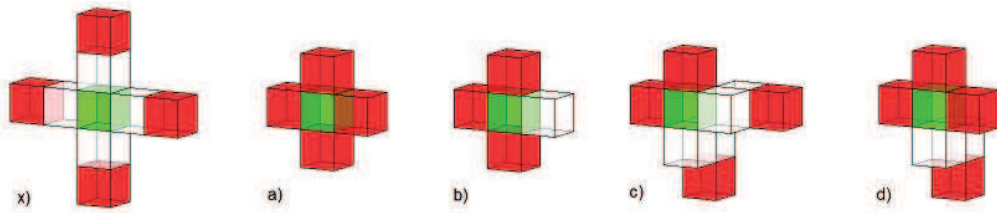

Figure 5: Structuring elements that provide boundary face relations between polygons and their 1−faces.
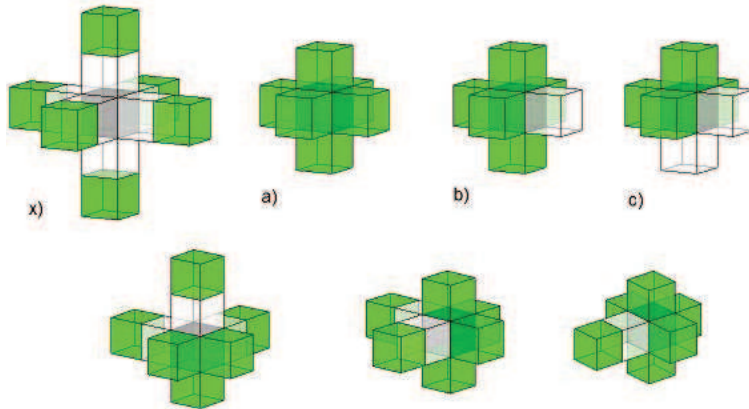

Figure 6: Structuring elements that provide boundary face relations between polyhedra and their 2−faces.

Observe that $Q(I)$ is constructed by adding unit cubes σ centered at points $r_\sigma = (i, j, k) \in \mathbb{Z}^3$. Therefore, the possible coordinates of r_μ for the ℓ-faces μ of σ are:

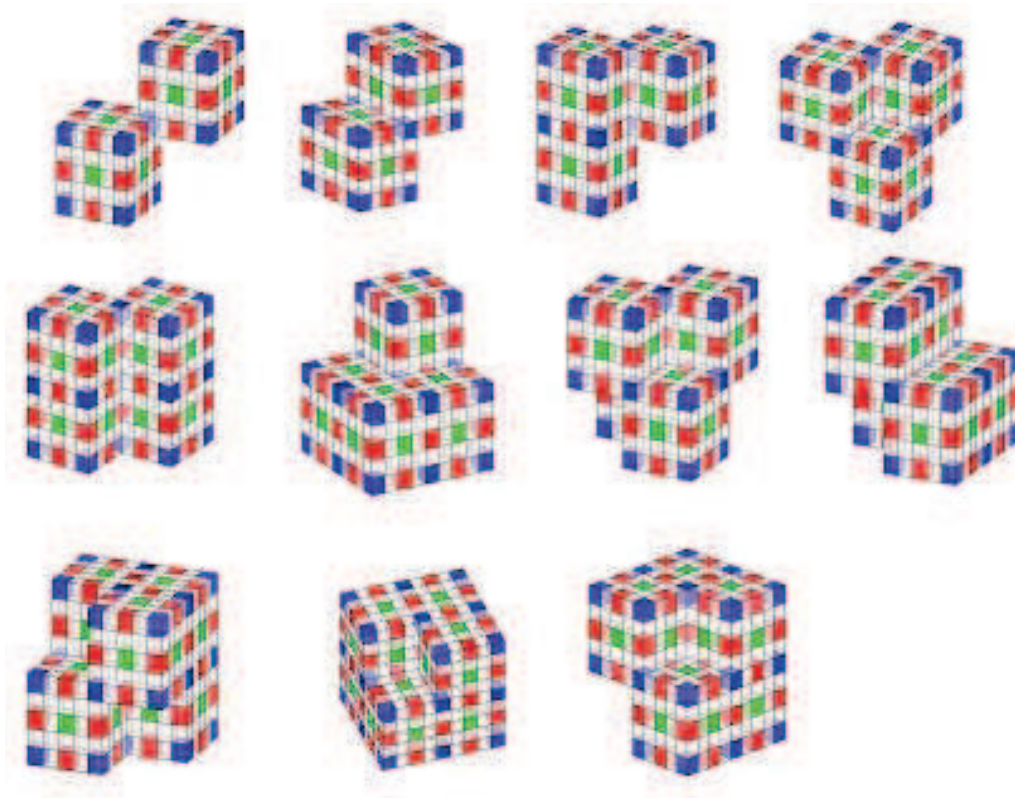- $(i \pm \frac{1}{2}, j \pm \frac{1}{2}, k \pm \frac{1}{2})$ if $\ell = 0$;

Figure 7: The color values in the ECM representations E_Q for the 3D complete cubical complexes corresponding to the eleven $8-$cube configurations around a critical vertex showed in Fig. 1.

- $(i, j \pm \frac{1}{2}, k \pm \frac{1}{2})$, $(i \pm \frac{1}{2}, j, k \pm \frac{1}{2})$ or $(i \pm \frac{1}{2}, j \pm \frac{1}{2}, k)$, if $\ell = 1$;

- $(i \pm \frac{1}{2}, j, k)$, $(i, j \pm \frac{1}{2}, k)$ or $(i, j, k \pm \frac{1}{2})$, if $\ell = 2$;

Proof. Since for any $\sigma \in Q(I)$, r_σ has either integer or multiple-of$-\frac{1}{2}$ coordinates, then $p = 4r_\sigma \in \mathbb{Z}^3$. More specifically,

- p represents a cube in $Q(I)$, if and only if $p = (4i, 4j, 4k)$;

- p represents a square face in $Q(I)$, if and only if either $p = (4i + 2, 4j, 4k)$, $p = (4i, 4j + 2, 4k)$ or $p = (4i, 4j, 4k + 2)$;

- p represents an edge in $Q(I)$, if and only if either $p = (4i+2, 4j+2, 4k)$, $p = (4i, 4j + 2, 4k + 2)$ or $p = (4i + 2, 4j, 4k + 2)$;

11

- p represents a vertex in $Q(I)$, if and only if $p = (4i + 2, 4j + 2, 4k + 2)$;

where $i, j, k \in \mathbb{Z}$. Besides, g_Q, by definition, relates each point $p \in D_Q$ representing a cell $\sigma \in Q(I)$ with the dimension of σ. Observe that b_ℓ, $\ell = 1, 2$, and their $90-$degree rotations describe six structural elements. For each $\ell-$cell $\sigma \in Q(I)$, $\ell = 1, 2$, only one of the three b_ℓ is associated to σ, depending on which axis the cell (edge or square face) is parallel to. b_3 is associated to the $3-$cells of $Q(I)$. Now, we have to prove that for each cell $\sigma \in Q(I)$, there exists a single structuring element $b_\sigma \in B_Q$ satisfying the conditions in Def. 3. We will prove this just for an edge parallel to the $x-$axis, since the proof for the rest of the cells is analogous. Suppose that $\sigma = e(u, v)$ is a unit edge with endpoints $u = (i - \frac{1}{2}, j + \frac{1}{2}, k + \frac{1}{2})$ and $v = (i + \frac{1}{2}, j + \frac{1}{2}, k + \frac{1}{2})$ (where $i, j, k \in \mathbb{Z}$). Then, $p_\sigma = (4i, 4j + 2, 4k + 2)$, $p_u = (4i - 2, 4j + 2, 4k + 2)$ and $p_v = (4i + 2, 4j + 2, 4k + 2)$. Therefore, $b_\sigma = b_1 : D_1 \to \mathbb{Z}$ since:

- $b_1(o) = 1 = g_Q(p_\sigma)$,
  $b_1((\pm 1, 0, 0)) = g_Q((4i \pm 1, 4j + 2, 4k + 2)) = -1$
  $b_1((\pm 2, 0, 0)) = g_Q((4i \pm 2, 4j + 2, 4k + 2)) = 0$.

- If $p = p_\mu$ represents an $(i-1)-$face of σ, then either $\mu = u$, and $b_1(p_u - p_\sigma) = b_1((-2, 0, 0)) = 0$; or $\mu = v$ and $b_1(p_v - p_\sigma) = b_1((2, 0, 0)) = 0$. Besides, if $p \in \mathbb{Z}^3$ such that $b_1(p - p_\sigma) = 0$, then $p - p_\sigma = (\pm 2, 0, 0)$ and therefore $p = p_u$ or $p = p_v$.

□

See Fig. 7 as an example of the color values in the ECM representations E_Q for several 3D complete cubical complexes $Q(I)$.

Remark 2. *The coface relations between cells can also be codified in terms of structuring elements in the ECM representation. More specifically, given a vertex $v \in Q(I)$ and its corresponding point p_v in the ECM representation E_Q, all the points representing the cofaces of v (see Fig. 8) can be found using a structuring element in the set $B_Q^c = \{b_\ell^c : D_\ell^c \to \mathbb{Z}\}_{\ell=1,2,3}$, where D_ℓ^c and $b_\ell^c : D_\ell^c \to \mathbb{Z}$ (modulo $90-$degree rotations) are given by:*

- $D_1^c = \{o, (1, 0, 0), (2, 0, 0)\}$;
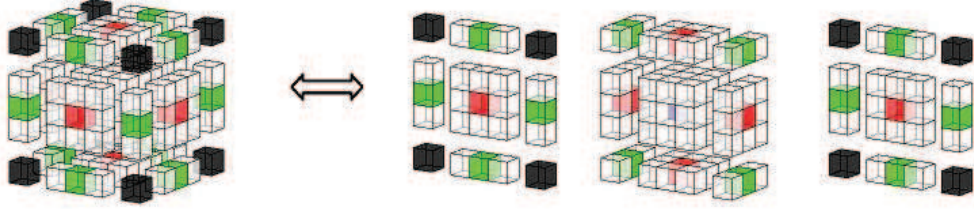 $b_1^c(o) = 0$, $b_1^c((1, 0, 0)) = -1$ *and* $b_1^c((2, 0, 0)) = 1$;

12

Figure 8: Color values of the voxels representing the cofaces of a vertex v when v is shared by 8 cubes.

- $D_2^c = \{o, (1,1,0), (2,2,0)\}$;
  $b_2^c(o) = 0$, $b_2^c((1,1,0)) = -1$ and $b_2^c((2,2,0)) = 2$.

- $D_3^c = \{o, (1,1,1), (2,2,2)\}$;
  $b_2^c(o) = 0$, $b_2^c((1,1,1)) = -1$ and $b_2^c((2,2,2)) = 3$.

Proposition 3. *Given the ECM representation E_Q of a cubical complex $Q(I)$ associated to a binary 3D digital image I, consider the set of structuring elements $B_Q^{critical} = \{b^{critical} : D^{critical} \to \mathbb{Z}\}$ showed in Fig. 9 (modulo reflections and $90-$degree rotations) and described below:*

- $D^{critical} = \{o, (\pm 1, \pm 1, \pm 1), (\pm 2, \pm 2, \pm 2)\}$;

- $b^{critical}(o) = 0$, $b^{critical}((\pm 1, \pm 1, \pm 1)) = -1$ and $b^{critical}((\pm 2, \pm 2, \pm 2))$ is either 3 or -1 (see Fig. 9).

A point $p \in \mathbb{Z}^3$ represents a critical vertex in $Q(I)$ if and only if a structuring element $b^{critical} \in B_Q^{critical}$ fits around p.

Proof. Consider the 8−cube configuration around a vertex showed in upper-left corner of Fig. 1. Suppose that a vertex $v = (i + \frac{1}{2}, j + \frac{1}{2}, k + \frac{1}{2})$ is shared by exactly two unit cubes c_1 and c_2 such that $r_{c_1} = (i, j, k)$ and $r_{c_2} = (i+1, j+1, k)$, where $i, j, k \in \mathbb{Z}$. Then $p_v = h_Q^{-1}(v) = (4i + 2, 4j + 2, 4k + 2)$, $p_{c_1} = h_Q^{-1}(c_1) = (4i, 4j, 4k)$ and $p_{c_2} = h_Q^{-1}(c_2) = (4i + 4, 4j + 4, 4k)$. Now consider the structuring element $b_1^{critical}$ depicted in Fig. 9.(upper-left). Points in $D_1^{critical}$ for which $b_1^{critical}$ takes value 3 are $p_1 = (-2, -2, -2)$ and $p_2 = (2, 2, -2)$. Let us check that $b_1^{critical}$ fits around p_v:

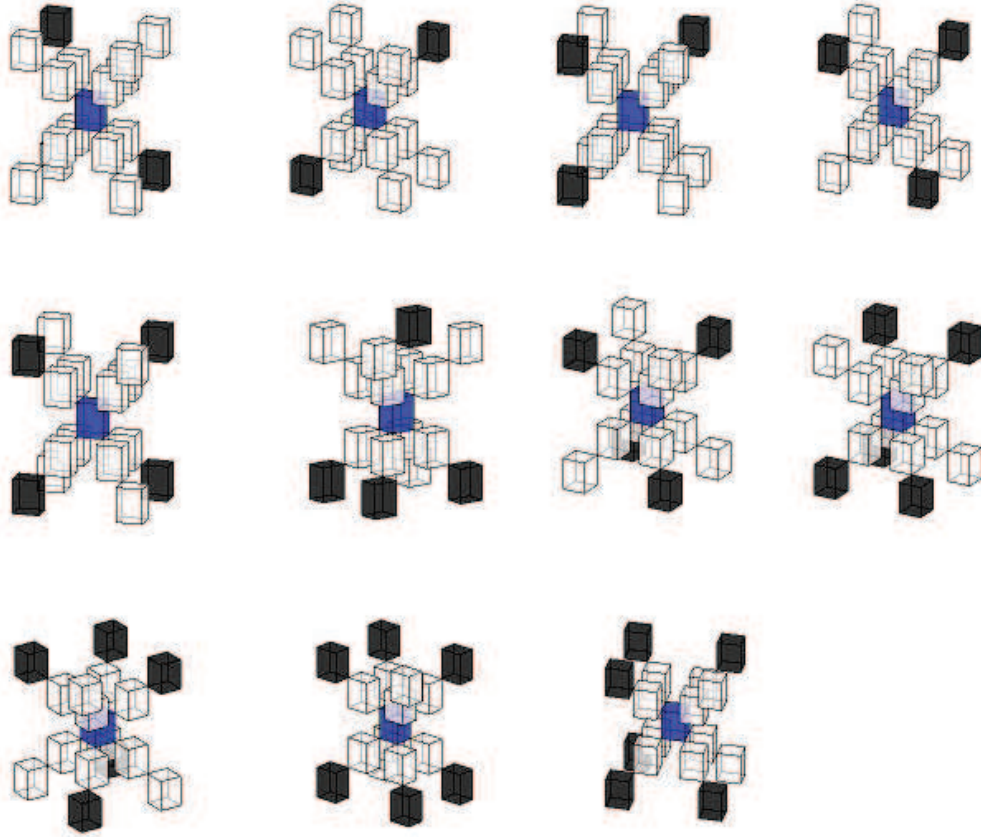- $b_1^{critical}(o) = 0 = g_Q(p_v)$;

13

Figure 9: Structuring elements (modulo reflections and 90−degree rotations) for the eleven 8−cube configurations around a critical vertex in $Q(I)$ showed in Fig. 1.

- $b_1^{critical}(p_1) = 3 = g_Q(4i, 4j, 4k)$; $b_1^{critical}(p_2) = 3 = g_Q(4i+4, 4j+4, 4k)$;

- $b_1^{critical}(p) = -1 = g_Q(p + p_v)$, for $p \in \{(\pm 1, \pm 1, \pm 1), (\pm 2, \pm 2, \pm 2)\} \setminus \{p_1, p_2\}$, since $\frac{1}{4}(p + p_v)$ does not correspond to the barycenter of any cell in $Q(I)$.

The rest of the configurations can be proven using similar arguments than above. □

14

4 Repairing the Critical Vertices on the ECM Representation E_Q of $Q(I)$

In this section, given the cubical complex $Q(I)$ (associated to a 3D image I) and the ECM representation E_Q of $Q(I)$ from Prop. 2, we show how to obtain the ECM representation $E_P = (h_P, g_P, B_P)$ of a well-composed polyhedral complex $P(I)$ homotopy equivalent to $Q(I)$. The "repairing" process that will be explained below consists of running over all the points $p \in \mathbb{Z}^3$ that represent critical vertices $v \in Q(I)$ and accomplishing a color-changing operation by modifying the values of g_Q in a neighborhood of p. New set of structuring elements, B_P, is then defined to codify the boundary relations between cells in $P(I)$.

Let $\ell = 1, 2$. The following sets of points in $\mathbb{Z}^3$ will be useful for different descriptions of points inside the ECM representation E_P:

- $N_6^\ell = \bigcup_{i=1,2,3}\{(x_1, x_2, x_3) \in \mathbb{Z}^3 \text{ s.t. } |x_i| = \ell \text{ and } x_j = 0 \text{ for } j \neq i\}$.

- $N_{12}^\ell = \bigcup_{i=1,2,3}\{(x_1, x_2, x_3) \in \mathbb{Z}^3 \text{ s.t. } x_i = 0 \text{ and } |x_j| = \ell \text{ for } j \neq i\}$.

- $N_8^\ell = \{(x_1, x_2, x_3) \in \mathbb{Z}^3 \text{ s.t. } |x_i| = \ell \text{ for } i = 1, 2, 3\}$.

- $N^\ell = \bigcup_{i=1,2,3}\{(x_1, x_2, x_3) \in \mathbb{Z}^3 \text{ s.t. } |x_i| = \ell \text{ and } |x_j| \leq \ell \text{ for } j \neq i\}$.

- $N^{\leq \ell} = \{(x_1, x_2, x_3) \in \mathbb{Z}^3 \text{ s.t. } |x_i| \leq \ell, i = 1, 2, 3\}$.

Finally, for a set $N \subset \mathbb{Z}^3$ and a point $p \in \mathbb{Z}^3$, let us denote by $N(p)$ the set $\{q + p \text{ such that } q \in N\}$.

Observe that $N^{\leq 1} = \{o\} \cup N^1$ and $N^{\leq 2} = \{o\} \cup N^1 \cup N^2$. In fact, given a point $p \in \mathbb{Z}^3$, $N^{\leq \ell}(p)$ is the $(2\ell + 1) \times (2\ell + 1) \times (2\ell + 1)$ block of voxels in $\mathbb{Z}^3$ centered at point p. If we consider this block as a big cube C_p composed by $(2\ell + 1)^3$ unit cubes, then:

- $N^\ell(p)$ are the faces of such a cube C_p.

- $N_6^\ell(p)$ are the 6 endpoints of the 3 segments with mid-point in p, length equal to $2\ell + 1$, and parallel to the coordinate axes.

- $N_{12}^\ell(p)$ are the (totally 12) vertices of the 3 squares centered at p, edge-length equal to $2\ell + 1$, parallel to the coordinate planes, and whose edges are parallel to coordinate axes.

- $N_8^\ell(p)$ are the vertices of the cube C_p.

The following remark ensures that given a point $p \in \mathbb{Z}^3$ such that $g_Q(p) = 0$ (which corresponds to a vertex $v = h_Q(p) \in Q(I)$), the modification of the map g_Q on the points in $N^{\leq 2}(p)$ only affects to points that either represent cofaces of v or do not represent any cell in $Q(I)$.

Remark 3. *Let $p \in \mathbb{Z}^3$ such that $g_Q(p) = 0$. Let $v = h_Q(p)$ be the corresponding vertex in $Q(I)$.*

- *If $q \in N^{\leq 2}(p) \setminus (N_6^2(p) \cup N_{12}^2(p) \cup N_8^2(p))$ then $g_Q(q) = -1$*

- *If $q \in N_6^2(p)$, then either $g_Q(q) = 1$ (q represents a $1-$coface of v) or $g_Q(q) = -1$.*
  Analogously, if $q \in N_{12}^2(p)$, then either $g_Q(q) = 2$ (q represents a $2-$coface of v) or $g_Q(q) = -1$.
  Finally, if $q \in N_8^2(p)$, then either $g_Q(q) = 3$ (q represents a $3-$coface of v) or $g_Q(q) = -1$.

See, for example, Fig. 8, which is an example of the values of g_Q on the set $N^{\leq 2}(p)$ where p represents a vertex shared by eight cubes in $Q(I)$.

Now, the following method is performed on the ECM representation E_Q to construct a new map $g_P : \mathbb{Z}^3 \to \mathbb{Z}$.

Procedure 1. *Start with the ECM representation $E_Q = (h_Q, g_Q, B_Q)$ of a given cubical complex $Q(I)$.*

0. *Initially, $g_P(p) = g_Q(p)$ for any $p \in \mathbb{Z}^3$.*

1. *Compute the set $R \subseteq \mathbb{Z}^3$ where $p \in R$ if $g_Q(p) = 0$ and one of the structuring elements showed in Fig. 9 fits around p (that is, $h_Q(p) \in Q(I)$ is a critical vertex).*

2. *For each point $p \in R$:*

   - *Compute the set $ST_p \subseteq \mathbb{Z}^3$ such that $q \in ST_p$ if one of the structuring elements given in Remark 2 fits around q (that is, $h_Q(q)$ is a cell in $St\{h_Q(p)\}$).*

   - *$g_P(p) = 3$;*
     $g_P(q) = 2$ if $q \in N_6^1(p)$;
     $g_P(q) = 1$ if $q \in N_{12}^1(p)$;
     and $g_P(q) = 0$ if $q \in N_8^1(p)$.
     See Fig. 10.a.

16

- *For each point $q \in ST_p$ such that $g_Q(q) = 1$, let $q_1 \in D_Q$ represent the other endpoint of q different to p. Then:*
  $g_P(q) = 3$;
  $g_P(s) = 2$ if $s \in N_6^1(q) \setminus (N^1(p) \cup N^1(q_1))$;
  and $g_P(s) = 1$ if $s \in N_{12}^1(q) \setminus (N^1(p) \cup N^1(q_1))$;
  See Fig. 10.b.

- *For each point $q \in ST_p$ such that $g_Q(q) = 2$, let $q_1, q_2, q_3, q_4 \in D_Q$ represent the 1-faces of the cell represented by q. Then:*
  $g_P(q) = 3$;
  and $g_P(s) = 2$ if $s \in N_6^1(q) \setminus (N^1(q_1) \cup N^1(q_2) \cup N^1(q_3) \cup N^1(q_4))$;
  See Fig. 10.c.

Notice that the points $q \in ST_p$ representing cubes in $Q(I)$ remain with the same color value, that is, $g_P(q) = 3 = g_Q(q)$. The above procedure could be improved by computing the sets R and $\{ST_p : p \in R\}$ at once, since the coordinates of the different cofaces of a point p representing a critical vertex in $Q(I)$ are known. For the sake of clarity we have separated the seeking of critical vertices (the set R) and their cofaces (the set ST_p for each p).

Proposition 4. *The map $g_P : \mathbb{Z}^3 \to \mathbb{Z}$ is well-defined.*

Proof. Observe that the 3D space $\mathbb{Z}^3$ can be decomposed into the following non-overlapping subspaces (see Fig. 8):

$$
\begin{aligned}
S_0 &= \{ \quad (4i + 2 \pm \ell_1, 4j + 2 \pm \ell_2, 4k + 2 \pm \ell_3) \}_{i,j,k \in \mathbb{Z}, \ell_1, \ell_2, \ell_3 \in \{0,1\}} \\
S_1 &= \{ \quad (4i + 2 \pm \ell_1, 4j + 2 \pm \ell_2, 4k), (4i + 2 \pm \ell_1, 4j, 4k + 2 \pm \ell_2), \\
&\qquad (4i, 4j + 2 \pm \ell_1, 4k + 2 \pm \ell_2) \}_{i,j,k \in \mathbb{Z}, \ell_1, \ell_2 \in \{0,1\}} \\
S_2 &= \{ \quad (4i + 2 \pm \ell, 4j, 4k), (4i, 4j + 2 \pm \ell, 4k), \\
&\qquad (4i, 4j, 4k + 2 \pm \ell) \}_{i,j,k \in \mathbb{Z}, \ell \in \{0,1\}} \\
S_3 &= \{ \quad (4i, 4j, 4k) \}_{i,j,k \in \mathbb{Z}}
\end{aligned}
$$

Then, color-changing process corresponding to a point $q \in \mathbb{Z}^3$ with $g_Q(q) = i$, for $i = 0, 1, 2, 3$, is performed on $S_i \cap N^{\leq 1}(q)$. In fact, the colors of all the points in $S_i \cap N^{\leq 1}(q)$ are modified.

Let $q_1, q_2 \in \mathbb{Z}^3$ be points with $i_1 = g_Q(q_1) \neq -1$ and $i_2 = g_Q(q_2) \neq -1$. The subsets $S_{i_1} \cap N^{\leq 1}(q_1)$ and $S_{i_2} \cap N^{\leq 1}(q_2)$ never intersect since:

- $N^{\leq 1}(q_1) \cap N^{\leq 1}(q_2) = \emptyset$ if $i_1 = i_2$,

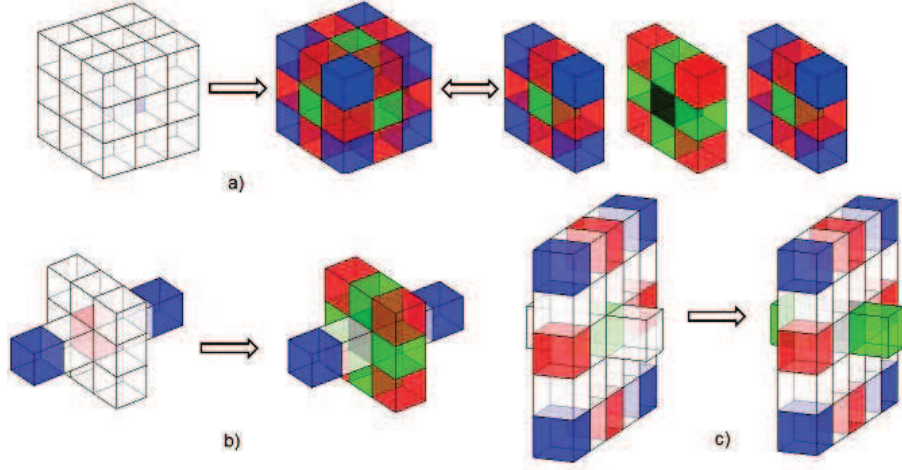- $S_{i_1} \cap S_{i_2} = \emptyset$ if $i_1 \neq i_2$.

Figure 10: a), b) and c) Illustration of the three color-changing operations on g_Q to obtain g_P.
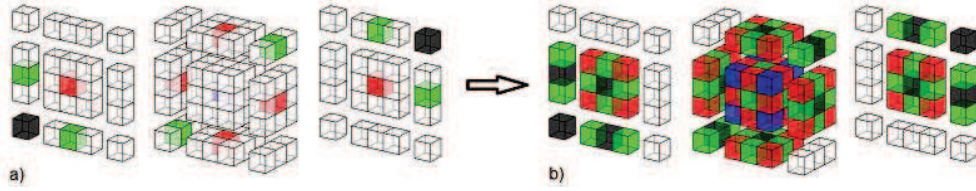

Figure 11: Color changing operation around a point representing the critical vertex in the top-left critical configuration of Fig. 1.

□

Fig. 10 illustrates the different color-changing operations described in Proc. 1. In Fig. 11.a, the color values of the ECM representation E_{Q_1} of the cubical complex Q_1 represented on the top-left of Fig. 1, are shown. Fig. 11.b shows the color values obtained after performing Proc. 1 on E_{Q_1}.

Now, we construct a new polyhedral complex $P(I)$ and a correspondence h_P between points with color values $g_P(p) \neq -1$ and cells of $P(I)$, in a way that $g_P(p) = dim(h_P(p))$. Any point $p \in \mathbb{Z}^3$ with $g_P(p) = 3$ will represent a polyhedron such that its faces will be represented by points in its neighborhood $N^{\leq 2}(p)$. Later, we will define a set of structuring elements B_P for which (g_P, h_P, B_P) is an ECM representation of $P(I)$.

The following polyhedra will be used in the construction of the polyhedral
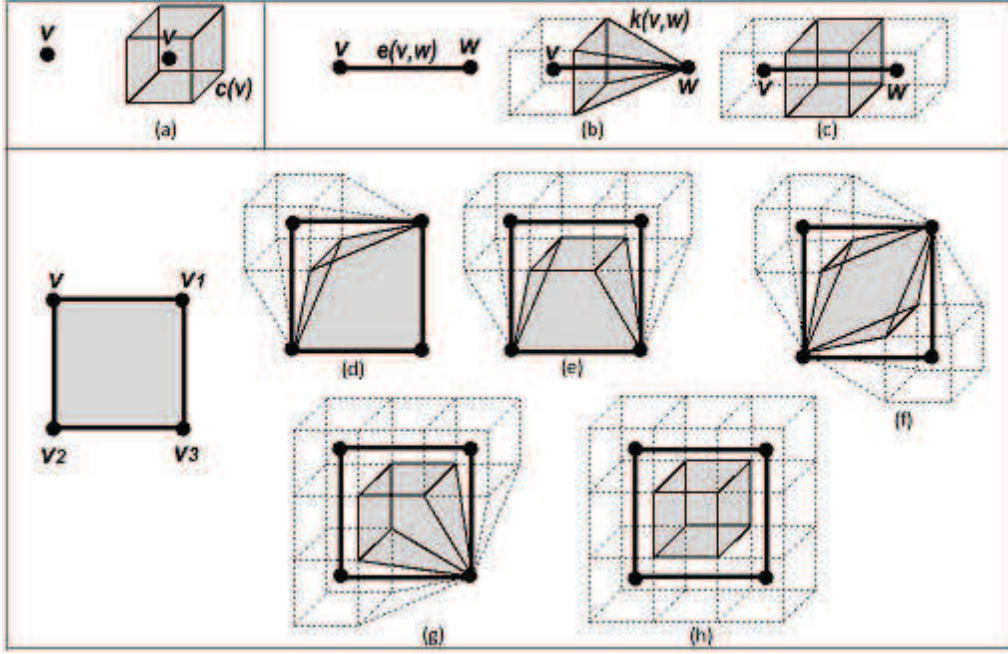
Figure 12: New polyhedra created in $P(I)$ associated with a vertex $v \in Q(I)$, a unit edge $e \in Q(I)$ with endpoints v and w and a unit square $s \in Q(I)$ with $0-$faces v, v_1, v_2 and v_3.

complex $P(I)$, that will be homotopy equivalent to $Q(I)$.

(a) The size$-\frac{1}{2}$ cube $c(v)$ centered at point $v \in \mathbb{R}^3$, with faces parallel to the coordinate planes. See Fig. 12.a.

(b) The pyramid $k(v, w)$ with apex a point w and base the square-face of $c(v)$ whose barycenter lies on the edge $e(v, w)$ with endpoints v and w. See Fig. 12.b.

(c) The polyhedra $\{p_i(v, v_1, v_2, v_3)\}_{i=1,2,3,4}$ (where v, v_1, v_2, v_3 are four distinct points in $\mathbb{R}^3$ forming a unit square s) given as follows:

  − $p_1(v, v_1, v_2, v_3)$ is determined by the triangles $t(v, v_1)$ and $t(v, v_2)$, and the edges $e(v_1, v_3)$ and $e(v_2, v_3)$ where $t(v, v_i)$, $i = 1, 2$, is the triangle face of $k(v, v_i)$ whose barycenter lies on the square s. See Fig. 12.d.
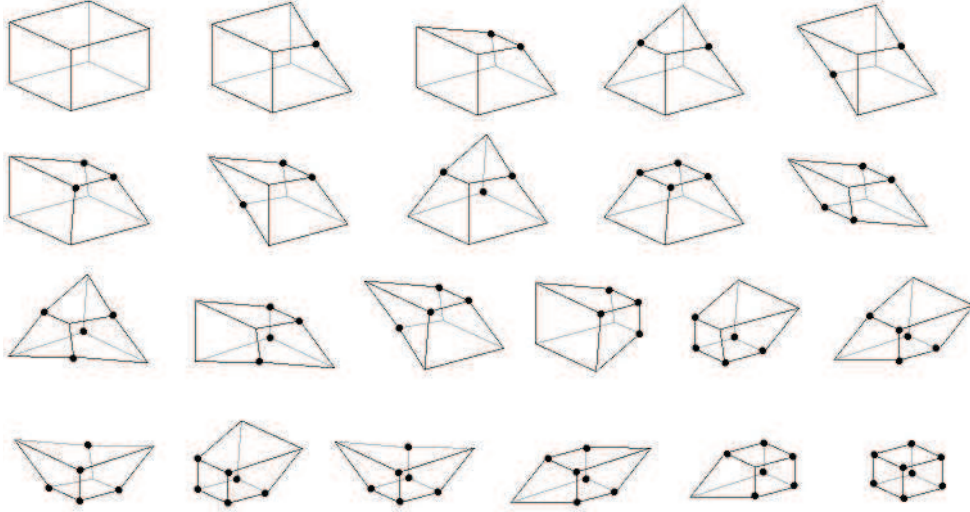
Figure 13: List of the hexahedra that can appear in $P(I)$. Each point in bold represents the vertex of $c(v_i)$, for some $i = 1, \ldots, 8$, which lies inside the cube $c(v)$.

- $p_2(v, v_1, v_2, v_3)$ is determined by the triangles $t(v, v_2)$ and $t(v_1, v_3)$, the square $s(v, v_1)$ and the edge $e(v_2, v_3)$, where $s(v, v_1)$ is the square face of $c(\frac{v+v_1}{2})$ whose barycenter lies on the square s. See Fig. 12.e.

- $p_3(v, v_1, v_2, v_3)$ is determined by the four triangles $t(v, v_1)$, $t(v, v_2)$, $t(v_3, v_1)$ and $t(v_3, v_2)$. See Fig. 12.f.

- $p_4(v, v_1, v_2, v_3)$ is determined by the squares $s(v, v_1)$ and $s(v, v_2)$ and the triangles $t(v_1, v_3)$ and $t(v_2, v_3)$. See Fig. 12.g.

- The 22 hexahedra $\{h_i(v_1, v_2, \ldots v_8)\}_{i=1,\ldots,22}$ (where $v_1, v_2 \ldots, v_8 \in \mathbb{R}^3$ form a unit cube c centered at a point $v \in \mathbb{Z}^3$, with faces parallel to the coordinate planes) showed in Fig. 13. In this picture, each bolded point represents the vertex of $c(v_i)$, for some $i = 1, \ldots, 8$, which lies inside the cube c. For example, the hexahedron on the top-left is c and the one on the bottom-right is the size$-\frac{1}{2}$ cube $c(v)$.

The sets of data $\{E_\alpha = (h_\alpha, g_\alpha, B_\alpha)\}_{\alpha=A,B,D,E,F,G}$ described below are ECM representations of the above polyhedra, whenever the coordinates of the vertices of the polyhedra are multiple of $\frac{1}{2}$.

(a) $D_A = N^{\leq 1}(p)$ for $p = 4v$.

$g_A(p) = 3$; $g_A(q) = 2$ if $q \in N_6^1(p)$; $g_A(q) = 1$ if $q \in N_{12}^1(p)$; $g_A(q) = 0$ if $q \in N_8^1(p)$ and $g_A(q) = -1$ if $q \in \mathbb{Z}^3 \setminus D_A$. See Fig. 14.a.

$h_A(p) = c(v)$; and $h_A(q) = \sigma$ if σ is a face of $c(v)$ and $q = 4r_\sigma$.

Structuring elements (modulo $90-$degree rotations) in B_A are showed in Fig. 6.a, Fig. 5.a and Fig. 4.a.

(b) $D_B = \{q\} \cup N^{\leq 1}(r) \setminus N^1(q)$ where $q = 4w$ and $r \in \mathbb{Z}^3$ is the closest point to $4r_{k(v,w)}$.

$g_B(r) = 3$; $g_B(q) = 0$; $g_B(s) = 2$ if $s \in N_6^1(r) \cap D_B$; $g_B(s) = 1$ if $s \in N_{12}^1(r) \cap D_B$; $g_B(s) = 0$ if $s \in N_8^1(r) \cap D_B$; and $g_B(s) = -1$ if $s \in \mathbb{Z}^3 \setminus D_B$. See Fig. 14.b.

$h_B(r) = k(v,w)$; $h_B(q) = w$; and $h_B(s) = \sigma$ if σ is an i-face of $k(v,w)$, and $s \in D_B$ is the closest point to $4r_\sigma$ such that $g_B(s) = i$.

Structuring elements (modulo $90-$degree rotations) in B_B are showed in Fig. 6.b, Fig. 5.b and Fig. 4.(a,b).

(c) The values of g_α for the rest of the ECM representation E_α, $\alpha = D, E, F, G$, are showed, respectively, in Fig. 14.(d, e, f, g).

The values of h_α are defined in an analogous way as above.

Structuring elements (modulo $90-$degree rotations) in B_α, $\alpha = D$, E, F, G, are showed in Fig. 6.c, Fig. 5.(c,d) and Fig. 4.(a,b).

The following procedure constructs the polyhedral complex $P(I)$ and the map $h_P : D_P \to P(I)$.

Procedure 2. *Let E_Q be the ECM representation of $Q(I)$ from Prop. 2. Let $g_P : \mathbb{Z}^3 \to \mathbb{Z}$ the output of Proc. 1. Let $D_P = \{p \in \mathbb{Z}^3 : g_P(p) \neq -1\}$. Let R be the set of points in $\mathbb{Z}^3$ representing the critical vertices in $Q(I)$. Let ST_p, $p \in R$, be the set of points in $\mathbb{Z}^3$ representing the cells in $St\{h_Q(p)\}$ (these sets were computed in Proc. 1).*
Initially, $P(I) = Q(I)$, and $h_P(p) = h_Q(p)$ for any $p \in \mathbb{Z}^3$.
For each $p \in R$,

- *Replace $v = h_Q(p) \in P(I)$ by the cube $c(v)$ together with all its faces. See Fig. 12.a. Define $h_P|_{D_A} = h_A$ where $D_A = N^{\leq 1}(p)$ and h_A is described above.*
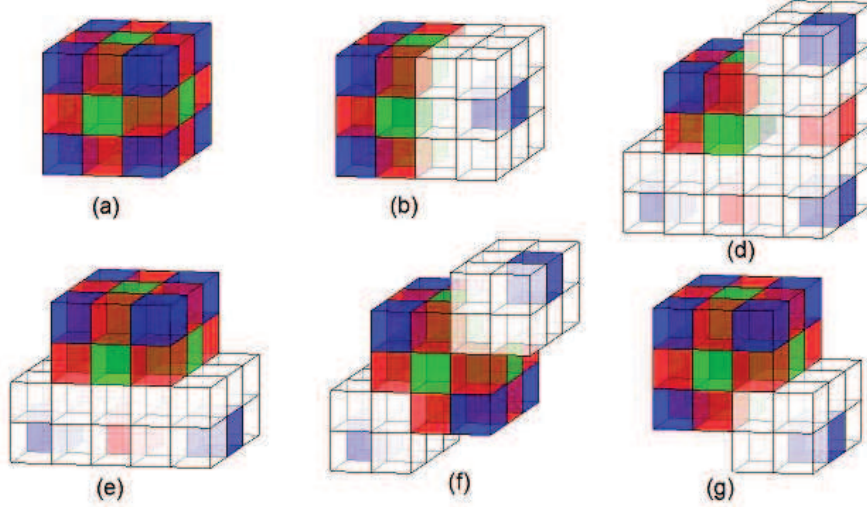
21

Figure 14: The color values in the ECM representations E_α, $\alpha = A, B, D, E, F, G$, of the polyhedra (and all their faces) described in Fig. 12.

- For each $r \in ST_p$ such that $g_Q(r) = 1$, let $v, w \in Q(I)$ represent the endpoints of $e(v, w) = h_Q(r)$.

  - If w is non-critical:
    * Replace $e(v, w) \in P(I)$ by the pyramid $k(v, w)$ together with its triangular faces. See Fig. 12.b;
    * Define $h_P|_{D_B} = h_B$.
  - If w is critical:
    * Replace $e(v, w) \in P(I)$ by the cube $c(\frac{v+w}{2})$, together with its faces parallel to $e(v, w)$. See Fig. 12.c.
    * Define $h_P|_{D_A} = h_A$ where $D_A = N^{\leq 1}(r)$.

- For each $r \in ST_p$ such that $g_Q(r) = 2$, let $v, v_1, v_2, v_3 \in Q(I)$ represent the $0-$faces of $\sigma = h_Q(r) \in Q(I)$ (see Fig. 12.left). Let $p_i = h_Q^{-1}(v_i)$ for $i =, 2, 3$.

  - If v_1, v_2, v_3 are non-critical,
    * Replace $\sigma \in P(I)$ by the polyhedron $p_1(v, v_1, v_2, v_3)$ together with its quadrangular faces. See Fig. 12.d.

22

∗ *Define $h_P|_{D_D} = h_D$.*

– *If v_1 is critical but v_2 and v_3 are not,*

∗ *Replace $\sigma \in P(I)$ by the polyhedron $p_2(v, v_1, v_2, v_3)$ together with its quadrangular faces sharing the edge $e(v_2, v_3)$. See Fig. 12.e.*

∗ *Define $h_P|_{D_E} = h_E$.*

An analogous case is when v_2 is critical but v_1 and v_3 are not.

– *If v_3 is critical but v_1 and v_2 are not,*

∗ *Replace $\sigma \in P(I)$ by the polyhedron $p_3(v, v_1, v_2, v_3)$ together with its quadrangular faces. See Fig. 12.f.*

∗ *Define $h_P|_{D_F} = h_F$.*

– *If v_1 and v_2 are critical but v_3 is not,*

∗ *Replace $\sigma \in P(I)$ by the polyhedron $p_4(v, v_1, v_2, v_3)$ together with its quadrangular faces sharing v_3. See Fig. 12.g.*

∗ *Define $h_P|_{D_G} = h_G$.*

– *If v_1, v_2 and v_3 are critical,*

∗ *Replace $\sigma \in P(I)$ by the cube $c(\frac{v+v_1+v_2+v_3}{4})$ together with its square faces parallel to σ (see Fig. 12.h.).*

∗ *Define $h_P|_{D_A} = h_A$ where $D_A = N^{\leq 1}(r)$.*

• *For each $r \in ST_p$ such that $g_Q(r) = 3$, the 3-cell $\sigma = h_Q(r)$ is replaced by a 3-cell μ which is one of the hexahedra showed in Fig. 13 depending on the number and positions of the critical vertices that are faces of σ. Define $h_P(r) = \mu$.*

Theorem 1. *$P(I)$ is a well-composed polyhedral complex homotopy equivalent to $Q(I)$.*

Proof. Let us prove that the polyhedral complex $P(I)$ is well defined:

• By construction, all the faces of each cell in $P(I)$ are also in $P(I)$.

• The intersection of any two cells of $P(I)$ is also a cell of $P(I)$, since during Proc. 2, each critical vertex v is replaced by $c(v)$ (together with all its faces) in $P(I)$ and each cell in $St\{v\}$ is replaced by a new polyhedron (together with its faces). Besides, all the faces of the polyhedron

23

added at each step are used in the next steps as faces of the new added polyhedra. Finally, an hexahedron of Fig. 13 substitutes the corresponding cube in $Q(I)$, whose faces are also faces of either previous cubes of $Q(I)$ or new polyhedra in $P(I)$.

- $P(I)$ is complete since the new added cells are always polyhedra together with all their faces.

Let us prove now that a homotopy equivalence (see [4]) from $P(I)$ to $Q(I)$ can be constructed. The key point is that, for each critical vertex $v \in Q(I)$, the cube $c(v) \in P(I)$ is homotopy equivalent to v. The homotopy equivalence is given by the projection of all the points in $c(v)$ onto v (in fact, it is a deformation retraction). The projection of the vertices of each cube $c(v)$ to v leads, in a natural way, to homotopy equivalences between the rest of the new constructed polyhedra in $P(I)$ and the corresponding cells of $Q(I)$:

- The pyramid $k(v,w)$ is homotopy equivalent to the edge $e(v,w)$, by the continuous function that maps the vertices of $s(v,w)$ (where $s(v,w)$ is the square face of $c(v)$ whose barycenter lies on $e(v,w)$) to v, and w to w; and it is extended continuously to all the points of the polyhedron;

- Analogously, the cube $c(\frac{v+w}{2})$ is homotopy equivalent to the edge $e(v, w)$, by the continuous function that maps $s(v,w)$ to v, and the ones of $s(w,v)$ to w.

- Each polyhedron $p_i(v, v_1, v_2, v_3)$ (see Fig. 12) is homotopy equivalent to the corresponding square with vertices v, v_1, v_2, v_3 by the continuous function that maps the vertices of $c(w)$ to w for $w = v, v_1, v_2, v_3$ if w is critical, or w to w if not. It is extended continuously to the rest of the points of the polyhedron

- Each hexahedron of quadrilateral faces (see Fig. 13) is homotopy equivalent to the corresponding unit cube obtained after mapping each size$-\frac{1}{2}$ cube $c(v)$ corresponding to a critical vertex $v \in Q(I)$, to v.

Finally the polyhedral complex $P(I)$ is well-composed. Observe that after performing Proc. 2, we have replaced each critical vertex $v \in Q(I)$ by a cube $c(v) \subseteq P(I)$, and the set $St\{v\} \subseteq Q(I)$ by $Stc(v) \subseteq P(I)$ (see, for example, Fig. 1 and Fig. 15). We have to prove that conditions $E1$ and $E2$ of Prop. 1 are satisfied:

24

(E1) Any edge $e = e(w_1, w_2)$ with endpoints w_1 and w_2 in $\partial P(I)$ has exactly two 2-cofaces:

- If e was also an edge in $\partial Q(I)$ satisfying $E1$, then neither w_1 nor w_2 were critical vertices and hence, e will have as 2-cofaces either square faces (that remain the same from $\partial Q(I)$) or quadrilateral faces of the polyhedra d) or e) of Fig. 12.

- If e is an edge of a cube $c(v)$ for some critical vertex v, then e has as 2-cofaces a square face of the cube $c(v)$ and either a triangular face of a pyramid $k(v, w)$ for some non critical vertex w, or a square face of a cube $c(\frac{v+w}{2})$ for some critical vertex w.

- If e is an edge of a pyramid $k(v, w_2)$ for some critical vertex v, then either e is shared by exactly two triangular faces of the pyramid, or it is shared by a triangular face of the pyramid and a quadrilateral face of a polyhedron $p_i(v, v_1, v_2, v_3)$ for some $i = 1, 2, 3, 4$, and $w_1 = v_j$ for some $j = 1, 2, 3$. See Fig. 12.(d-g).

(E2) For any vertex $w_1 \in \partial P(I)$, $Lk\{w_1\}$ in $\partial P(I)$ has exactly one connected component:

- If w_1 was also a vertex in $\partial Q(I)$ (that is, w_1 was a non-critical vertex and hence, satisfied condition $E2$), then $Lk\{w_1\}$ was a set of edges and vertices in $\partial Q(I)$, that are faces of $2-$cofaces of w_1. In the case that any of those $2-$cofaces were replaced by a polyhedron $p_i(v, v_1, v_2, v_3)$ for some $i = 1, 2, 3, 4$, some critical vertex v and such that $w_1 = v_j$ for some $j = 1, 2, 3$, only one of the quadrilateral faces f of $p_i(v, v_1, v_2, v_3)$ would lie on $\partial P(I)$ and the edges and vertices in $Lk\{w_1\}$ in $\partial Q(I)$ would be replaced by the edges and vertices of $c(v)$ and $k(v, w_1)$ shared with f. The way of construction of the new polyhedra guarantees that $Lk\{w_1\}$ in $\partial P(I)$ is still connected.

- If w_1 is a vertex of a cube $c(v)$ for some critical vertex v of $Q(I)$, then, by construction, the 2-cofaces of w_1 are either square faces of $c(v)$, or triangular faces of a pyramid $k(v, w)$, for some non-critical vertex w, or square faces of an adjacent cube $c(\frac{v+w}{2})$ for some other critical vertex w, or quadrilateral faces of the polyhedra $p_i(v, v_1, v_2, v_3)$ showed in Fig. 12. Then, $Lk\{w_1\}$ in $\partial P(I)$, as one can guess from Fig. 12, has exactly one connected component.
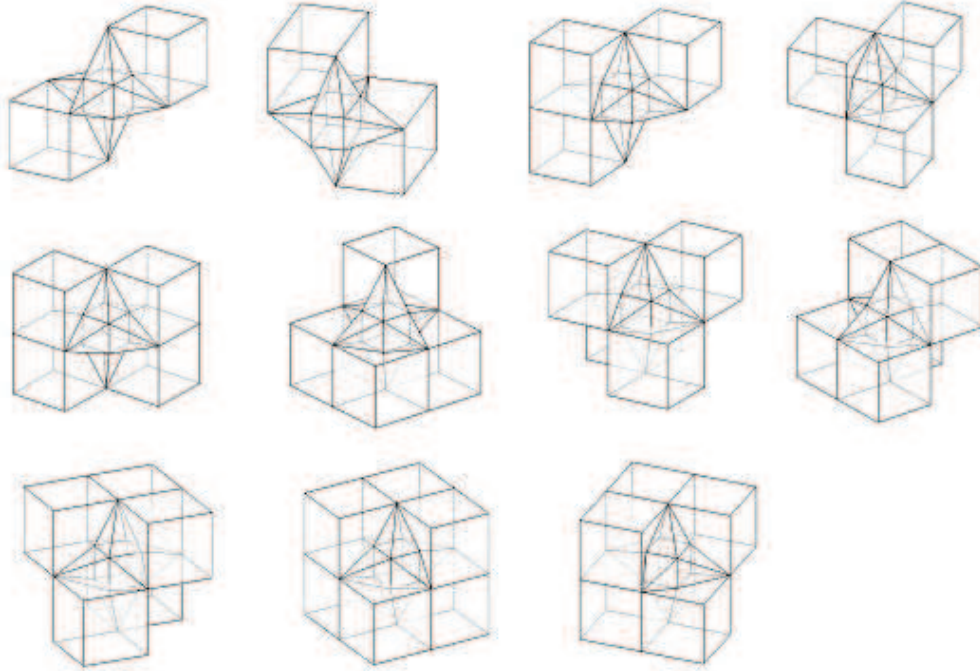
25

Figure 15: The well-composed polyhedral complexes obtained after performing Proc. 1 and Proc 2 **only on the central vertex for the 3D complete cubical complexes showed in Fig. 1.**

□

In Fig. 16.a, there is a simple example of a cubical complex $Q(I)$ associated to a 3D image composed by 6 voxels. The color values of the ECM representation E_Q of $Q(I)$ is showed in Fig. 17.a. The color values in E_P after performing the repairing process explained in Proc. 1 is showed in Fig. 17.b. In Fig. 16.b, there is the 3D well-composed polyhedral complex $P(I)$ obtained following Proc. 2.

Theorem 2. *The triple $E_P = (h_P, g_P, B_P)$ is an ECM representation of $P(I)$.*

Proof. Observe that $P(I)$ is constructed by replacing each cell in $Q(I)$ which is a coface of a critical vertex, by a particular polyhedron defined above. Observe that the color-values in the ECM representations E_α, $\alpha = A, B, D, E$, F, G, of each new added polyhedron in $P(I)$, used for computing the ECM
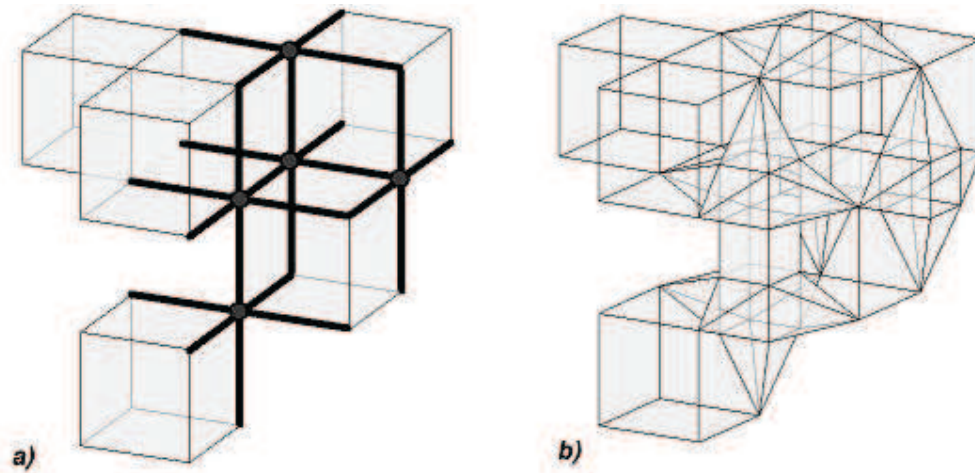
26

Figure 16: a) A cubical complex $Q(I)$ associated to a 3D image composed by 6 voxels. b) The obtained 3D well-composed polyhedral complex $P(I)$.
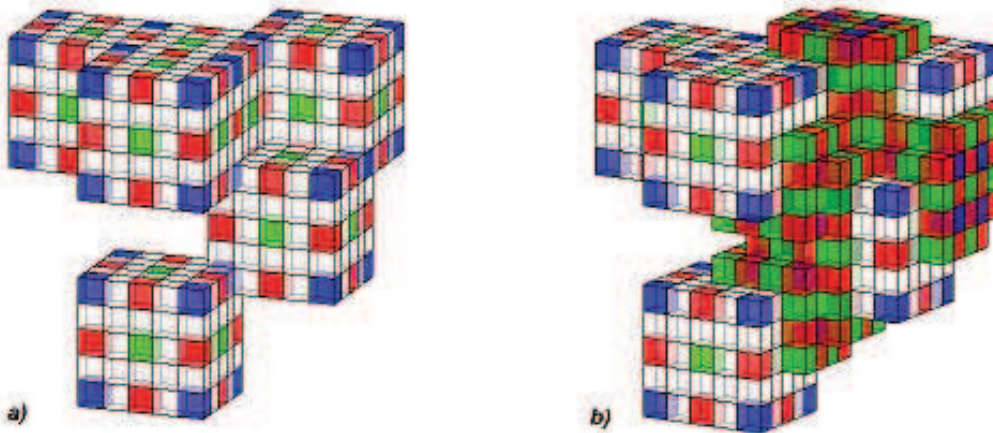

Figure 17: a) The color values in E_Q where $Q(I)$ is the cubical complex showed in Fig. 16.a. b) The color values in E_P after performing the repairing process explained in Proc. 1.

representation for $P(I)$, coincides with the color-values computed in Proc. 1. For this reason, for any $p \in D_P$, $g_P(p) = dim(h_P(p))$. Finally, the new structuring elements stored in B_P are obtained from the ECM representation of each new added polyhedra in Proc. 2. $\square$

5 Conclusion and Future Work

In this paper, we have presented a representation scheme called ECM representation for storage and manipulate the cells of both an initial cubical complex $Q(I)$ associated to a 3D digital image I and a 3D well-composed polyhedral complex homotopy equivalent to it. Using this scheme, we have presented a method for constructing the complex $P(I)$.

Although the representation of the final polyhedron is $64 = 4^3$ times bigger than the input, plus the space required to encode voxel colors, there are several advantages when using our approach as we will see below. In order to compute properties on a polyhedral complex K such as homology, we only need to store the map $g_K : \mathbb{Z}^3 \to \mathbb{Z}$ and the structuring elements B_K. However, the set B_P remain the same for any ECM representation E_P of $P(I)$ obtained from a cubical complex $Q(I)$ after performing Proc. 2. Therefore, Proc. 1 provides enough information to compute the homology of $P(I)$.

The overall method is linear in the number of cells of the initial cubical complex $Q(I)$. In fact, the method is linear in the number of critical vertices of $Q(I)$ and only the points in $N^{\leq 2}(p_v)$ (which represent the cells in $St\{v\}$ for any critical vertex v) are modified. Observe that the representation scheme could be improved, considering only the critical vertices of $Q(I)$ and their cofaces. Besides, we think that voxel colors may not be needed since the dimension of a cell $\sigma \in P(I)$ represented by a point $p \in \mathbb{Z}^3$ may be deduced from the coordinates of p. We let these last tasks for future work.

Finally, this way of representation provides a fast access to the cells of $Q(I)$ and $P(I)$, in terms of the coordinates used to codify it, as well as an efficient way to get all the boundary faces of each cell. And what is more important, to obtain all this information we do not need to build $P(I)$.

Future work could be to extend our method to nD and to adapt the existing algorithms developed in the context of well-composed images to well-composed polyhedral complexes.

References

[1] Artzy E., Frieder G., Herman G.T.: The theory, design, implementation and evaluation of a three-dimensional surface detection algorithm.

Comput. Graphics Image Process. 15, 1–24 (1981)

[2] Wagner H., Chen C., Vucini E.: Efficient computation of persistent homology for cubical data, in Topological Methods in Data Analysis and Visualization II, Mathematics and Visualization, 91–106 (2012) Proc. of the 4th Workshop on Topology-based Methods in Data Analysis and Visualization (TopoInVis 2011), 2011

[3] Computer Assisted Proofs in Dynamics: CAPD Homology Library, http://capd.ii.uj.edu.pl.

[4] Hatcher A.: Algebraic Topology. Cambridge University Press, Cambridge, 2002

[5] Herman G.T.: Discrete multidimensional Jordan surfaces. CVGIP, Graphical Models Image Process. 54, 507–515 (1992)

[6] Gonzalez-Diaz, R., Jimenez, M.J., Medrano, B.: Cubical cohomology ring of 3D photographs. Int. J. Imaging Syst. Technol. 21 (1), 76–85 (2011)

[7] Gonzalez-Diaz R., Umble R., Lamar-Leon J.: Cup products on polyhedral approximations of 3D digital images. In Proc. of the 14th Int. Conf. on Combinatorial image analysis (IWCIA'11). LNCS 6636, 107–119 (2011)

[8] Gonzalez-Diaz R., Jimenez M.J., Medrano B.: Well-composed cell complexes. In Proc. of the 16th IAPR Int. Conf. on Discrete geometry for computer imagery (DGCI'11). LNCS 6607, 153–162 (2011)

[9] Kovalevsky V.: Geometry of Locally Finite Spaces. Publishing House, Berlin, Germany (2008)

[10] Kozlov D.: Combinatorial Algebraic Topology. Algorithms and computation in maths 21, 2008

[11] Krahnstoever N., Lorenz C.: Computing curvature-adaptive surface triangulations of three-dimensional image data. Vis. Comput. 20 (1), 17–36 (2004)

[12] Lachaud J. O., Montanvert A.: Continuous analogs of digital boundaries: A topological approach to iso-surfaces. Graphical Models 62, 129–164 (2000)

[13] Latecki L.J., Eckhardt U., Rosenfeld A.: Well-composed sets. Comput. Vis. Image Underst. 61 (1), 70–83 (1995)

[14] Latecki L.J.: 3D Well-composed pictures. Graphical Models and Image Processing 59 (3), 164–172 (1997)

[15] Latecki L.J.: Discrete representation of spatial objects in computer vision. Kluwer Academic, Dordrecht, 1998

[16] Lorensen, W. E., Cline, H.E.: Marching cubes: A high resolution 3d surface construction algorithm. ACM Computer Graphics 21 (4), 163169 (1987)

[17] Marchadier J., Arques D., Michelin S.: Thinning grayscale well-composed images. Pattern Recognit. Lett. 25 (5), 581–590 (2004)

[18] Stelldinger P., Latecki L.J., Siqueira J.M.: Topological equivalence between a 3D object and the reconstruction of its digital image. IEEE Trans. Pattern Anal. Mach. Intell. 29 (1), 126–140 (2007)

[19] Stelldinger P.: Image digitization and its influence on shape properties in finite dimensions. IOS Press. 312 (2008)

[20] Rosenfeld A., Kong T.Y., Wu A.Y.: Digital surfaces. CVGIP, Graphical Models Image Process. 53, 305–312 (1991)

[21] Siqueira M., Latecki L.J., Tustison N., Gallier J., Gee J.: Topological repairing of 3D digital images. J. Math. Imaging Vis. 30, 249–274 (2008)